Damage in glass-concrete composite panels

Luigi Biolzi, Sara Cattaneo *, Pietro Crespi, Nicola Giordano

Department of Architecture, Built Environment and Construction Engineering, Politecnico di Milano, Piazza Leonardo da Vinci 32, 20133 Milano, Italy

The evolution of damage of a glass-concrete façade panel is presented and discussed. The phenomenon is strongly influenced by the mutual interaction between three materials (concrete, steel rebars and glass) having different mechanical and rheological properties.

To assess the possible causes of the observed damages, detailed 3D finite element numerical analyses were conducted considering the effects of thermal loads, due to difference of temperature outside and inside of the building, and the effects of concrete shrinkage. Furthermore, a construction stages analysis was implemented to consider the loading history during the production process of the panel.

The analyses were performed both in linear elastic and non-linear conditions to assess the stress redis-tributions in the panel due to concrete cracking. In particular, the analyses showed that the shrinkage of concrete was the main reason of the detected damage in a case study, even considering the creep that mitigates the phenomenon leading to a delayed cracking. Finally, a parametric study is presented assum-ing different factors (concrete rib sizes, different shrinkage laws, as a consequence of the addition of shrinkage-reducing admixtures (SRA), different bond between glass and concrete and different reinforce-ment ratio). The results of this parametric study suggest interesting remarks about suitable design prin-ciples of glass-concrete façade panels.

Keywords: Glass-concrete, Composite panels, Shrinkage, Thermal loads, Numerical model

Highlights:

Progressive failure analysis of glass concrete composite panels.
Simplified analytical model.
Failure prevention due to concrete shrinkage.
A case study.

1. Introduction

The research of high degrees of transparency has become a main concern in architecture following the increase of the application of glass in buildings. Therefore, from being used for simple infill panels, the glass is increasingly used to form complete load bearing structures. Among them, precast glass concrete panels have been employed as skylights, deck lights, stairs, landings, bridges, sidewalks, walls and other original uses. A surprising range of applications is conceivable with a resultant variety of aesthetic results [1].

Article history:
Received 2 November 2015
Received in revised form 10 April 2016
Accepted 26 April 2016

* Corresponding author.
E-mail addresses: luigi.biolzi@polimi.it (L. Biolzi), sara.cattaneo@polimi.it (S. Cattaneo), pietro.crespi@polimi.it (P. Crespi), nicola.giordano@polimi.it (N. Giordano).

The glass hollow blocks allow the reduction of supply costs with respect to traditional windows because they join the intrinsic characteristics of transparency with the worthwhile use of a modular element (for transportation, storage and on-site installation) [2]. In addition, the higher specific mass ensures a better sound insulation against impact noises and, the air chamber into the glass ensures a good thermal insulation. Glass is a homogeneous and isotropic material, having a linear elastic behavior up to a brittle failure [3]. The macroscopic strength of glass is dominated by microstructural flaws, which are always present, due to the production processes and subsequent handling. Furthermore, cutting processes negatively affect the mechanical response of glass elements, because of an additional defect production along the element boundaries that locally reduces the tensile strength [4]. The microcracks open in mode I when the tensile stress reaches a critical limit, but they can grow over time even for stress values much

Published Journal Article available at: http://dx.doi.org/10.1016/j.conbuildmat.2016.04.106

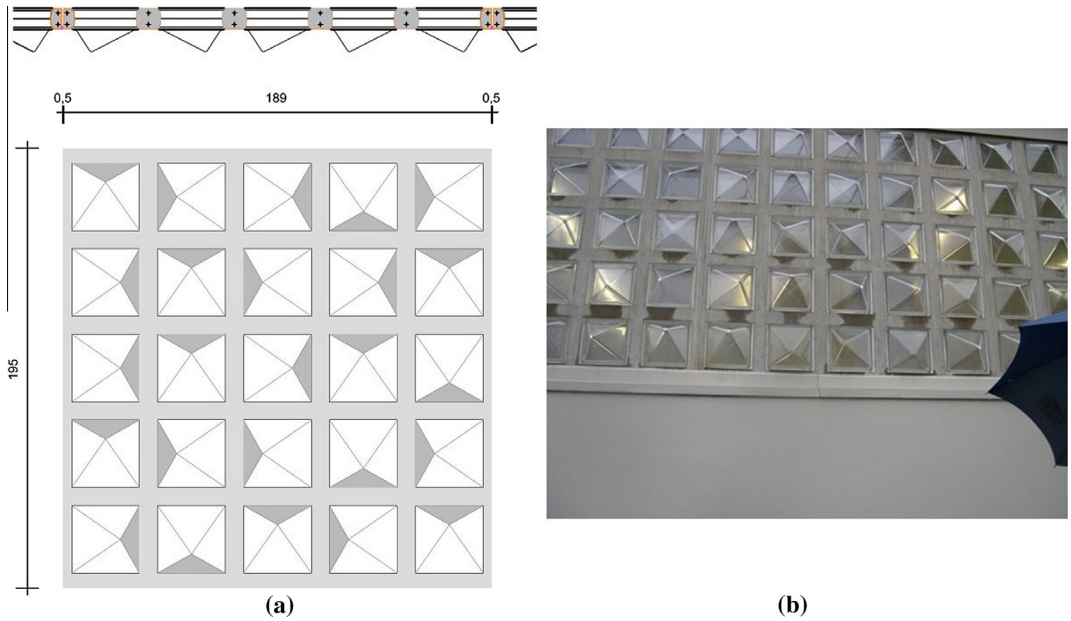

Fig. 1. (a) Panel 5 × 5 (measures in cm); (b) Portion of the façade.

Fig. 2. Damaged glass block and cracked concrete surface.

lower than the critical ones. This phenomenon, usually denoted as static fatigue or slow crack propagation, makes the glass strength dependent upon time and thermo-hygrometric conditions that, in turn, affect the speed of the slow crack propagation. In a composite panel, in addition to glass, there is also concrete, which has a peculiar long-term behavior. All concretes shrink, even the so-called shrinkage-compensating concrete, that is they show a time dependent strain. Concrete shrinkage strain persists to increase with time at a decreasing rate. Shrinkage reaches a final value as time approaches infinity and is dependent on all the factors which affect the drying of concrete, including the relative humidity, the temperature, the mix characteristics (type and quantity of the binder, water content, and water-to-cement ratio, ratio of fine to coarse aggregate, and the type of aggregate), and the size and shape of the element [5,6]. Because of a loss in volume, concrete shrinkage can lead to cracking when concrete is restrained [7]. Evident and/or unreasonably wide cracks usually may be unpleasant and spoil a visible concrete surface; in addition they allow the entrance of moisture thus accelerating corrosion of the reinforcement and leading to durability problems. Concrete shrinkage is an important design issue because it can cause, when restrained by a rigid glass element, an additional state of stress more and more significant in time. This paper is addressed to present and discuss the effects of a problematic combination of different materials, leading to irreversible damages of the glass-concrete composite panels with significant consequences on aesthetic, functional and economical aspects. The results of an extensive and detailed three dimensional finite element numerical analysis are illustrated. Linear and nonlinear analyses to evaluate the consequences of environmental thermal conditions and concrete shrinkage are presented as well. Even if the stress level was small, the creep effect was considered to evaluate whether it could significantly reduce the shrinkage effect. Finally, the influence of the concrete rib size, of the addition of SRA, of the bond between glass and concrete and of different reinforcement ratio were taken into consideration.

2. Observed damage

The problem of damage in glass-concrete composite panels is discussed with reference to an actual application of precast glass-concrete façade panels. The curtain wall, made of glass block concrete elements, was adopted in several façades of a complex building, with all exposures. Since the façades had different sizes, several types of panels were built, containing a different number of glass blocks, ranging from a minimum of 10 (panel size 189 × 86.5 cm) up to a maximum of 65 (panel size 189 × 493 cm).

The geometry of a panel with 25 blocks (5 × 5) and a portion of the façade is shown in Fig. 1.

A damage of the façade panels was observed just after the end of the construction works (about three months after the casting of the panels). In particular, some glass blocks showed a crack

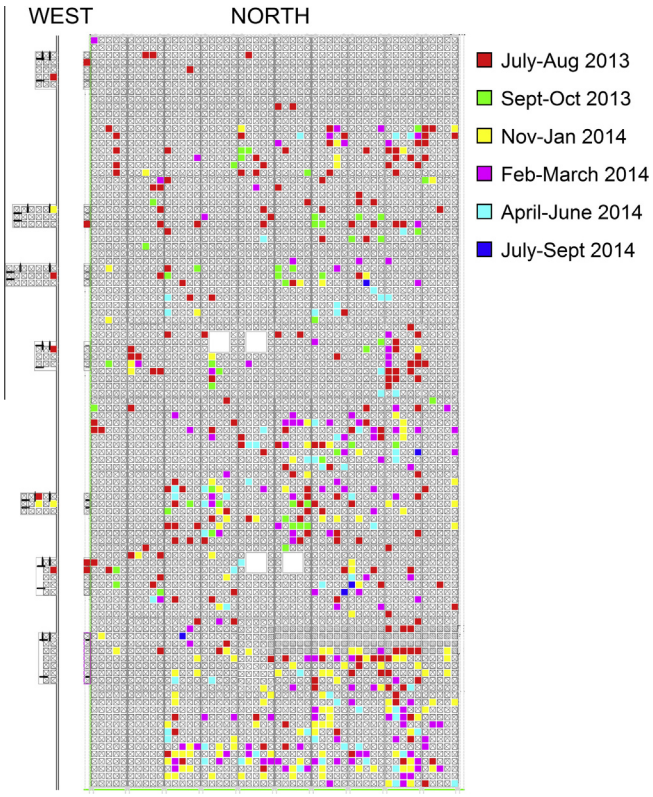

Fig. 3. Main façade of the building: geometry and evolution of damage.

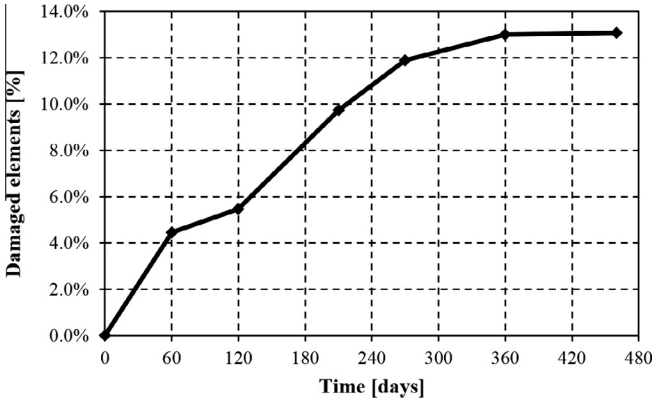

Fig. 4. Percentage of damaged blocks versus time.

on the inner surface as shown in Fig. 2. In some cases, the crack on the glass was related to a nearby crack on the concrete surface. Usually cracks developed around the middle of the side of the glass block (nothing was detected around the glass block corners) (Fig. 2).

The detected damage was randomly distributed whatever the exposure of the façade, the size of the panel and the position of the panel within the façade, as shown in Fig. 3 where the west and the north façade damages are shown. No significant differences in the damage distribution was detected.

The damage abruptly developed up to about one year later when the rate of damage of the glass block decreased, as shown in Fig. 4, where the percentage of damaged glass blocks versus time is plotted.

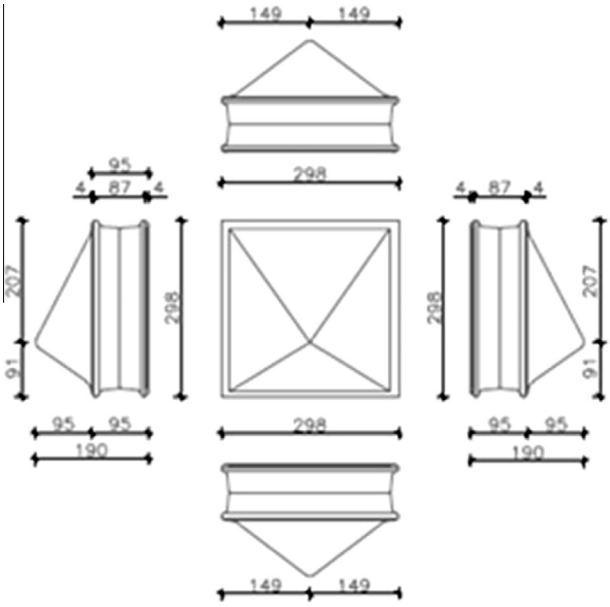

Fig. 5. Diamond-shaped glass block.

3. Materials

The concrete panels had a thickness of about 9.5 cm together with a distance between glass blocks of 8 cm. The concrete ribs were reinforced with two rebars (steel class B450C, according to European Standard [8], 8 mm diameter) as shown in Fig. 1. The concrete cover was about 15 mm. Two bushes were introduced to allow the handling of the panel.

3.1. Glass blocks

The glass blocks were obtained by coupling a plane element with a diamond shaped one. The detailed geometry of the glass block is shown in Fig. 5, the side length is about 300 mm.

The conformity assessment of the product was done according to EN1051-2 [9] while the evaluation of the thermal transmittance ($U_f = 1.4\ Wm^{-2}\ K^{-1}$) was done following EN 673 [10]. Compression tests according to EN1051-1 [11] were performed as well.

The compressive strength determined according to EN1051-1 Annex A (loaded surface 298 × 98 mm) was about 10 MPa (coefficient of variation of about 12.22%), while the tests according to EN1051-2 Annex E (determined over a 40 × 40 mm load surface) showed an average strength of 16.74 MPa (coefficient of variation of about 24.08%).

Additional tests according to EN1051-2 Annex B and EN ISO 7459 [12] were performed to evaluate the thermal shock resistance (assumed temperatures were 50 °C and 20 °C). All specimens did not show any damage.

3.2. Concrete

Concrete class C32/40 was selected for the production of glass-concrete composite panels. During the production, a CEMII/B-LL 42.5R cement was used and the maximum aggregate size was 16 mm. The compressive cubic strength measured after 460 days was 57.12 MPa, corresponding to 41.2 MPa at 28 days.

3.3. Connections

The connection between panels was achieved by using a vulcanized rubber with mechanical properties evaluated according to EN ISO 8339 [13]. This type of connection does not induce any additional stress.

The panels were connected to the structure by four hangers welded on-site to a tubular steel frame fixed to the reinforced concrete structures through post-installed bonded fasteners. Therefore, the panels are independent and subjected only to self-weight.

4. Environmental conditions

Environmental conditions (temperature and relative humidity) could be, among other factors, a cause of the observed damage.

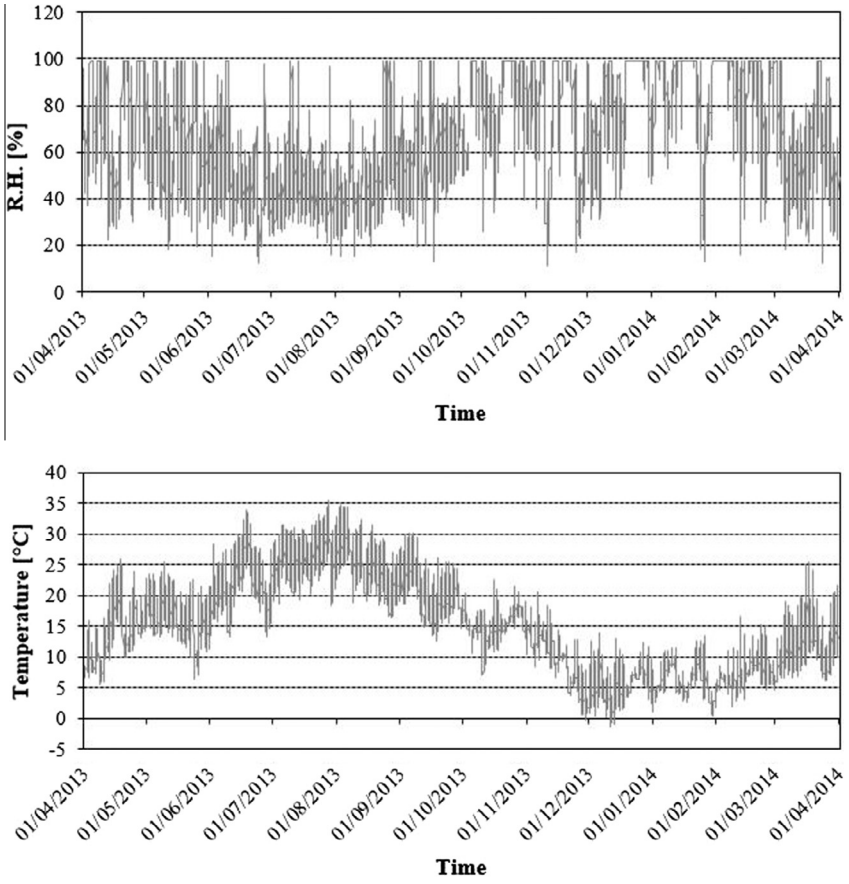

Fig. 6. Temperature and relative humidity over time.

For this reason, the collected data every hour for one year (in a weather station close to the building) by the Regional Agency have been considered (Fig. 6).

5. Linear elastic analytical model

A simple analytical model was formulated to evaluate the shrinkage effects over time.

Let us consider a portion of the concrete rib and the two halves of the nearby glass blocks (Fig. 7).

The shrinkage induces a deformation in the concrete $\varepsilon_C(t,t_{sh})$, where t is the time and t_{sh} is the time when structural effects of shrinkage begins.

The concrete is restrained by the glass and the reinforcement. Due to these restraints the concrete is subjected to a tensile stress and mutual actions between steel rebar and concrete $X_S(t,t_{sh})$ and glass and concrete $X_G(t,t_{sh})$ rise.

Due to equilibrium the force on the concrete $X_C(t, t_{sh})$ is equal to:

$$X_C(t,t_{sh}) = X_S(t,t_{sh}) + X_G(t,t_{sh}) \tag{1}$$

Assuming a linear elastic behavior of all materials the compatibility condition implies:

$$\varepsilon_{sh}(t,t_{sh}) = \frac{X_C(t,t_{sh})}{E_C A_c} + \frac{X_S(t,t_{sh})}{E_S A_S} + \frac{X_G(t,t_{sh})}{E_G A_G} \tag{2}$$

where E_C, E_S, E_G are the concrete, steel and glass elastic modulus and A_C, A_S, A_G are the corresponding areas.

According to the plane section hypothesis the strain in the three materials are the same:

$$\varepsilon_C(t,t_{sh}) = \varepsilon_S(t,t_{sh}) = \varepsilon_G(t,t_{sh}) \tag{3}$$

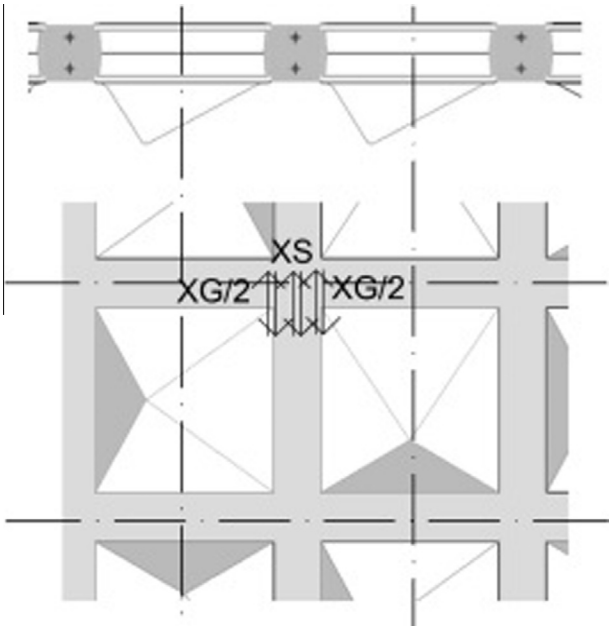

Fig. 7. Mutual forces between concrete and steel and between concrete and glass.

From Eqs. (1)–(3) it is possible to obtain the actions within concrete, glass and reinforcement and thus the corresponding stresses in the concrete rib $\sigma_C(t,t_{sh})$, in the glass $\sigma_G(t,t_{sh})$ and in the steel $\sigma_S(t,t_{sh})$ (which change over time depending on the shrinkage deformation) can be evaluated (Fig. 8).

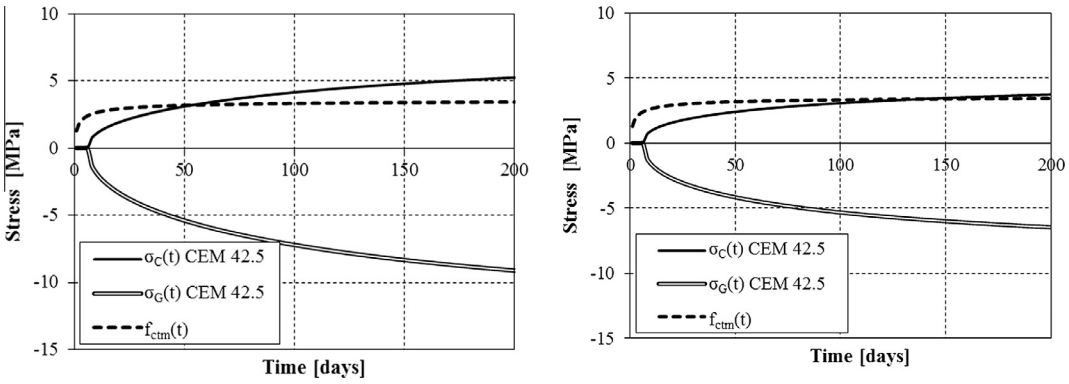

Fig. 8. Stresses within the concrete (σ_C) and the glass (σ_G) for concrete made with CEM42.5R concrete tensile strength (f_{ctm}) considering only shrinkage (left) or shrinkage and creep (right).

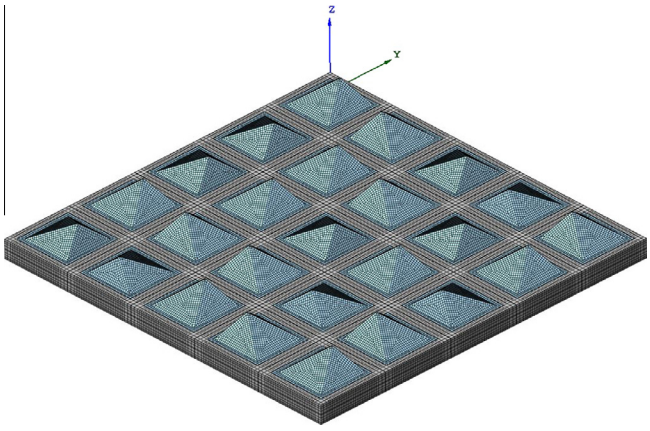

Fig. 9. Numerical FEM model of the panel.

For instance, the shrinkage law given by CEB Model Code 2010 [14] can be assumed as a reference, assuming a cement CEM 42.5R with a relative humidity of 67% (average value according to experimental data) and a time of beginning of shrinkage of 7 days (demoulding).

By considering the concrete tensile strength ($f_{ctm}(t)$) evaluated according to [14] it results that cracking appears after about 58 days (Fig. 8 left, intersection between f_{ctm} and σ_c). Obviously this result depends on the shrinkage law adopted, and on several factors (i.e. the actual tensile strength of the concrete) so it must not be considered a "true value", but it gives a reasonable value (according to in situ observation) in which the damage phenomena begun.

Nevertheless, even if creep in tension is still an open issue see e.g. [15–17], it is interesting to evaluate whether cracking could be avoided because of the relaxation due to creep. For this reason, according to the age adjusted effective modulus method, an aging coefficient χ equal to 0.8 and a creep coefficient ($\varphi(t,t_0)$) reported in CEB Model Code 2010 [14] were adopted, even if in [14] it is clearly stated that the proposed laws apply as well to concrete in tension, though those relations are directed towards the prediction of concrete creep subjected to compressive stresses.

By comparing the results with or without creep (Fig. 8) it is confirmed that creep mitigate the phenomenon of progressive glass block cracking, which is delayed (cracking at about 125 days) but not avoided.

Again, these results depend on the shrinkage/creep law adopted, and in this case it seems that the strong relaxation due to creep is not consistent with the timing of the observed damage.

When cracking occurs, this model does not apply anymore and non-linear behavior has to be accounted for.

6. Numerical model

To evaluate the causes and evolution of the damage, a numerical model of a representative glass-concrete panel has been considered (Fig. 9). The model accounted for the complex geometry considering a symmetric 189 × 195 cm size panel, with 5 × 5 glass-concrete single cells. The finite element model (FEM), using the commercial code MIDAS FEA, was composed by 3D tetrahedral and hexahedral elements within beam elements representing the reinforcing bars placed in the concrete ribs (for an overall number of 266,219 elements and 271,541 nodes). The model was fully constrained in 4 connection points and subjected to the self-weight load. The concrete shrinkage and temperature gradient effects due to the different temperatures between the indoor and outdoor sides of the building were considered as well.

A complete time-dependent linear elastic construction stage analysis was performed to simulate the loading sequence of the panel. Five construction stages were considered as described in Table 1.

During the first stage, the maximum tensile stress in the materials was about 0.1 MPa, significantly lower than their limit strength.

Table 1
Description of the 5 construction stages.

Stage	Time [days]	Panel position	Applied loads
1	0	Horizontal, fully supported	Self-weight
2	7	Horizontal, fully supported	Self-weight + shrinkage
3	7	Vertical, fully fixed in 4 points	Self-weight + shrinkage
4	180	Vertical, fully fixed in 4 points	Self-weight + shrinkage
5	180	Vertical, fully fixed in 4 points	Self-weight + shrinkage + winter thermal loading condition

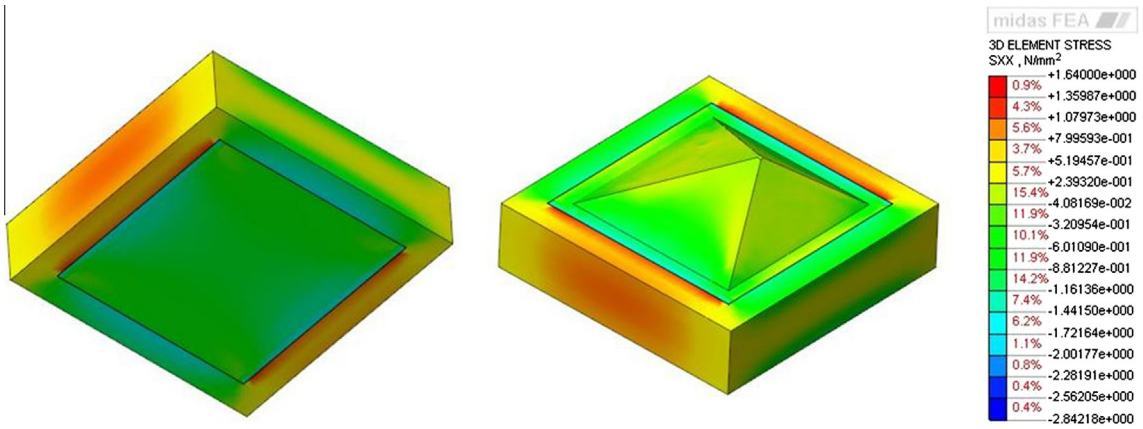

Fig. 10. Stage 2: normal stresses σ_{xx} in the central cell of the panel.

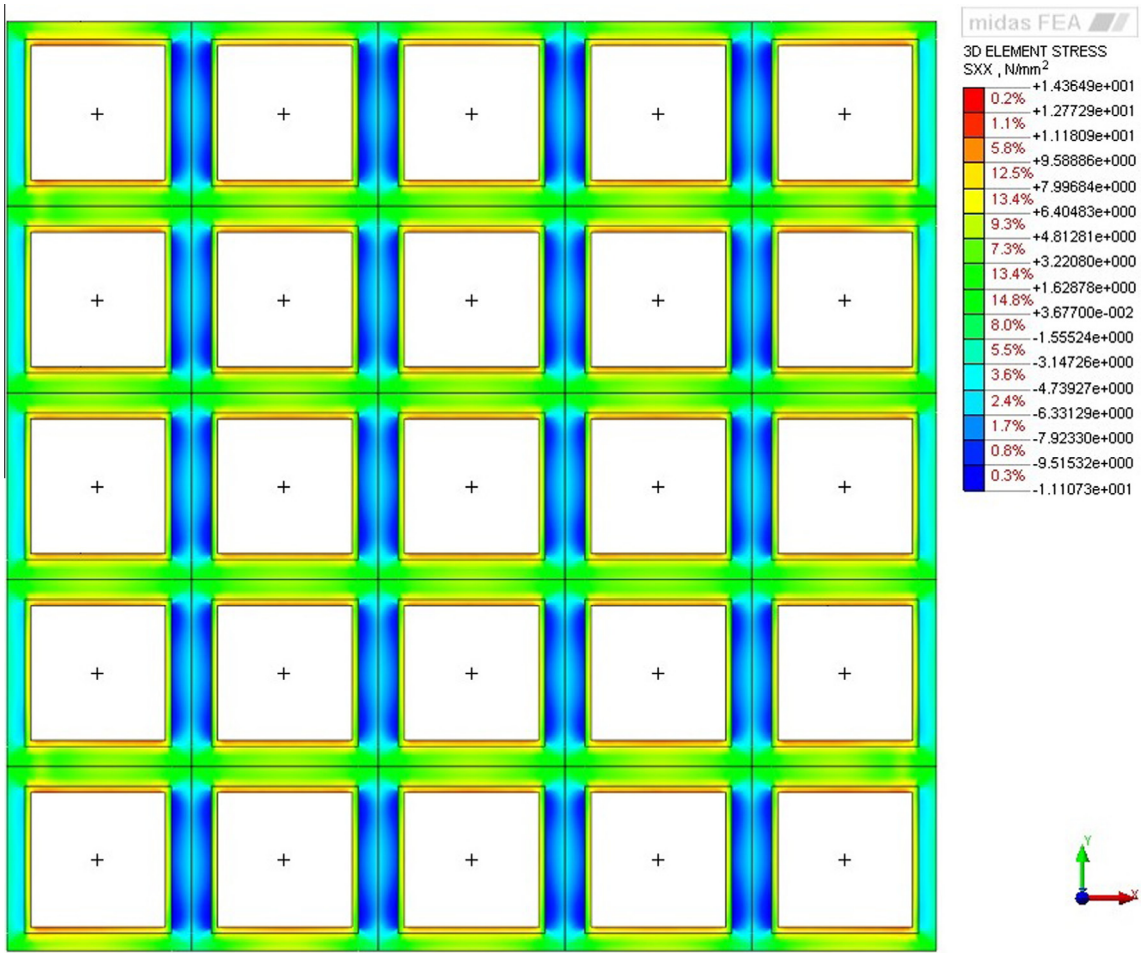

Fig. 11. Stage 4: normal stresses σ_{xx} in the concrete ribs of the panel.

At the end of the second stage (7 days) the first effects of shrinkage phenomenon were detected, with a maximum tensile stress in the concrete ribs that reached about 1.2 MPa. In any case the stress is still significantly lower than the concrete tensile strength evaluated as 3.02 MPa according to the Model Code 2010 [13]. At the same time, the glass blocks and the reinforcing bars were under a compression stress field. The normal stresses σ_{xx} contour in the single central cell of the panel is reported in Fig. 10.

At the end of the curing period (7 days) the panel was placed in vertical position (Stage 3), and higher stresses near the 4 connection points were detected.

The fourth stage considered the panel mounted on the façade after about 6 months. The effects of concrete shrinkage lead to significant increase of the stresses in the materials. In particular, the concrete has to be considered cracked, since a concrete tensile stress of 7.4 MPa was evaluated.

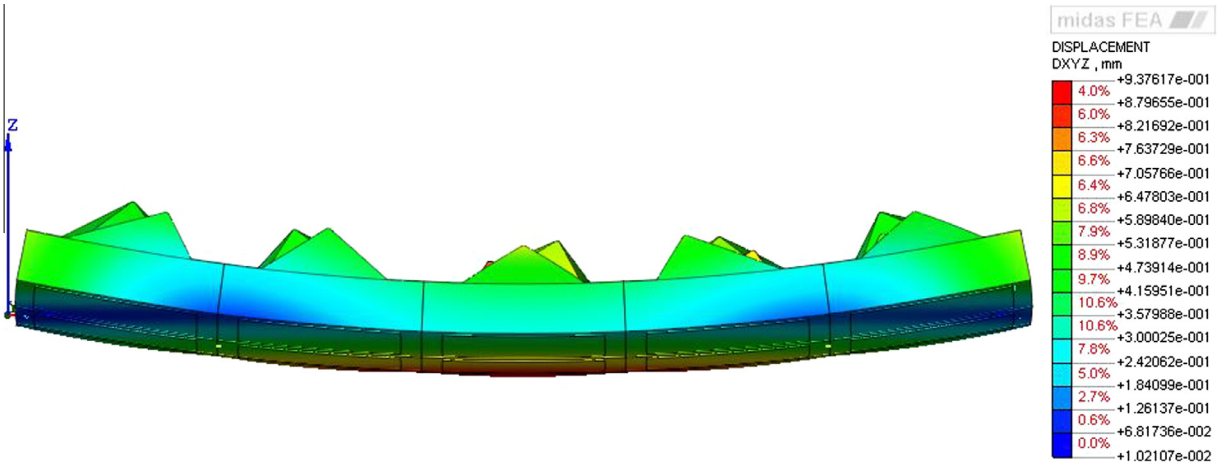

Fig. 12. Stage 5: deformed shape of the panel.

Table 2
Normal stresses in X-direction on the inner face of the central cell.

	$\sigma_{xx,GLASS}$ [MPa]	$\sigma_{xx,CONCRETE}$ [MPa]
Stage 3-Shrinkage 7 days	−1.73	1.06
Stage 4-Shrinkage 180 days	−6.66	7.21
Stage 5-Shrinkage 180 days + Thermal load	−5.29	8.04
Thermal load	1.37	0.83

At the end of this stage, the stress field in the concrete ribs of the panel is quite regular (Fig. 11); this is mainly because each panel does not interact with the adjacent ones.

Finally, in the last stage, the winter thermal loading (the most severe among those possible) was considered. The temperature distribution increased the displacements (Fig. 12) and stresses of the panel and the maximum concrete tensile stress in this stage was about 8 MPa.

According to the performed linear analysis, it seems that the first three phases were not critical for the observed damage phenomena but the effects of shrinkage at 180 days and thermal load condition seem to justify the evolution of the damage process, while the effect of constrains at the four corners was negligible.

In particular, the shrinkage strains at 180 days produce high tensile stresses in concrete (7.41 MPa) and, for equilibrium conditions, compression stresses in glass block elements. This stress level causes cracking in the concrete and, as a consequence, a complete stress redistribution into glass and steel rebars. After concrete cracking, glass is no longer compressed, and the tensile stresses could be critical and cause cracking in the glass blocks in the nearest point characterized by the presence of a surface defect.

The concrete and glass stresses on the inner face of the panel (at the interface between glass and concrete) are reported in Table 2.

A non-linear model for a single cell of the panel has been implemented to evaluate the stress field in cracked condition. In particular, interface elements having an elastic-brittle constitutive model have been introduced. Figs. 13 and 14 show the stresses in the rebar and in the cell before and after cracks development.

According to the linear elastic analysis, the stress field in the single cell of the panel is characterized by tensile stresses in concrete and compression in glass and steel rebars.

Due to concrete cracking, a change of the stress fields occurs: tensile stresses in glass block and in the neighborhood reach high values that may be unacceptable with the strength of float glass. At the end of the shrinkage process, the glass stresses increase until about 65 MPa. Furthermore, the plane face of the glass element is mostly compressed: this result justifies the limited propagation of the crack toward the block (Fig. 15). The stress concentration nearby the crack can be justified because of the perfect bond between concrete and glass.

7. Discussion

The problem is very complex to interpret with reliable predictions. Indeed, as shown in Fig. 11, the stress distribution is almost

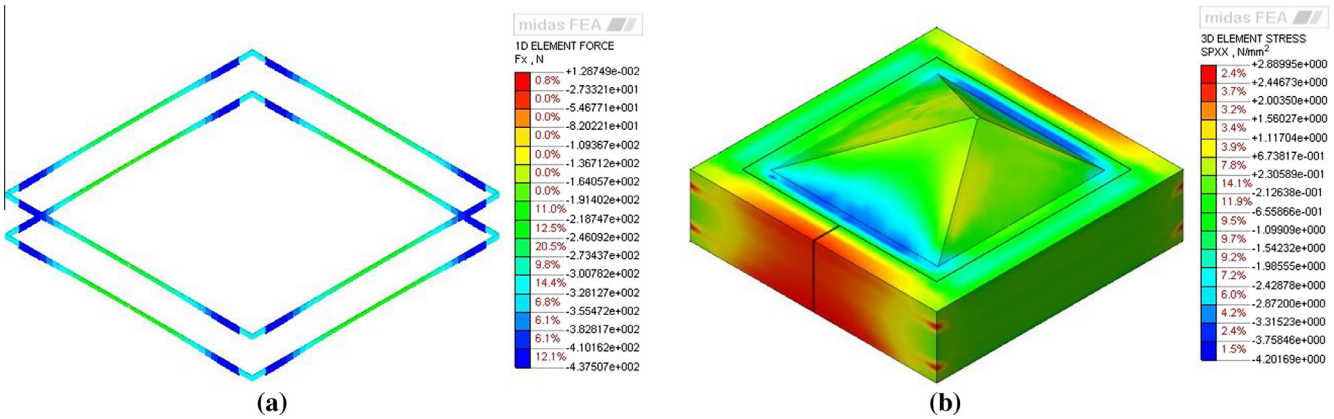

Fig. 13. Stresses field before cracks: (a) axial force in the rebars; (b) normal stresses σ_{xx}.

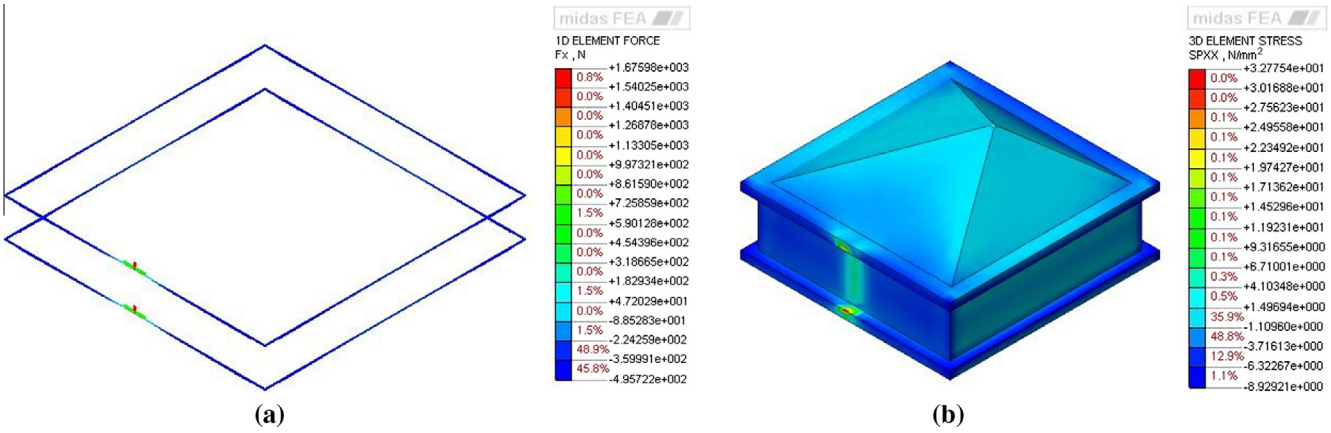

Fig. 14. Stresses field after cracks: (a) axial force in the rebars; (b) normal stresses σ_{xx}.

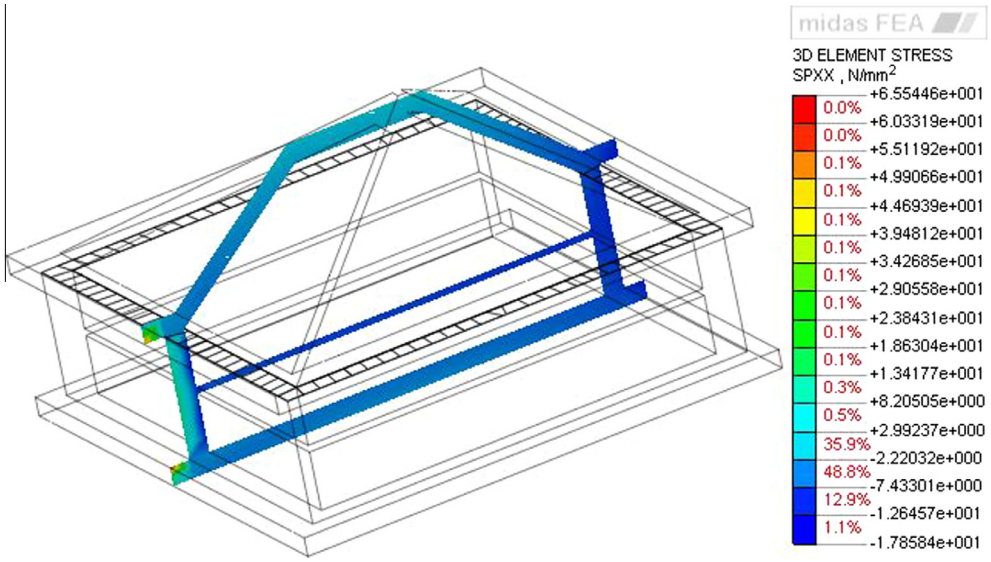

Fig. 15. Slice plane representation of normal stresses σ_{xx} inside the glass block.

uniform and the cracking phenomenon depends on the defects of both concrete and glass. In particular, since concrete is not an homogeneous material cracking does not happen anywhere but nearby a dominant defect. Once cracks develop in the concrete ribs, stress peaks in the glass blocks occur, and the subsequent cracking depends on the geometry of possible defects. If the glass block surface was without defects or made with tempered glass, the stress peaks produced by the cracking of the concrete would not be sufficient to trigger the observed cracking.

The numerical analyses showed that the behavior of the glass-concrete composite panels is affected by several factors.

Among them, the shrinkage appears to be the main factor that caused the damage, nevertheless other factors (i.e. size of the concrete rib, bond between glass and concrete and even the reinforcement ratio) play a primary role and have to be considered for a suitable design.

For this reason, additional numerical analyses have been performed to evaluate the effect of each parameter (shrinkage strain, size of the concrete rib, bond between glass and concrete, reinforcement ratio) that should influence the overall behavior of the panel.

To evaluate the influence of the panel geometry (in terms of concrete rib thickness) and the possible addition of SRA (Shrinkage Reduction Admixture) to reduce shrinkage [14], the linear elastic

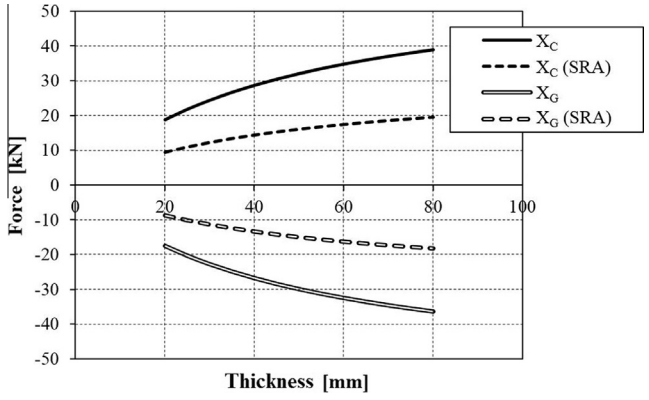

Fig. 16. Forces in concrete and glass with/without SRA as a function of the size of the concrete rib.

analytical model was considered to find the internal forces rising into both concrete and glass. Fig. 16 shows the axial forces as a function of the concrete rib size, and highlights that both parameters (size and SRA) strongly affect the results. Indeed, by considering the shrinkage strain at 180 days (continuous line), it can be

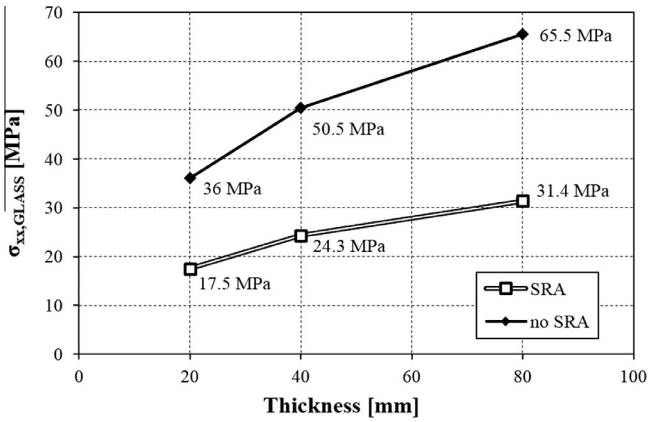

Fig. 17. Tensile stresses on glass block for different thicknesses and addition of SRA.

observed that the internal forces within the two materials are almost twice by considering a side of 80 mm instead of a side of 20 mm. By using a SRA in the concrete mix the shrinkage strain was reduced at 50% and thus, due to the linearity of the model the actions will be reduced of the 50% as well (dashed line).

On the basis of these results, additional numerical analyses had been performed considering different design conditions: with or without SRA and with three different sizes of the concrete rib. The obtained results in terms of normal stresses that can cause the damage on the inner face of the glass block are reported in Fig. 17.

It is clear that the addition of a proper amount of SRA allows to use larger size for concrete ribs, while without SRA, ribs no larger than 20 mm should be adopted, because the stresses appear already significant for a float glass with unavoidable surface defects.

Another way to modify the stress field in the panel, and in particular in the glass blocks, is to reduce the bond between concrete and glass blocks. To this end a suitable layer of soft material (e.g. polyurethane resins with poor mechanical properties) could be used between concrete and glass blocks.

To evaluate the possible difference in the case of a reduced bonding (between the two materials) the analyses have been repeated by introducing an interface between glass and concrete

Table 3
Effect of bond and reinforcement in glass block: maximum normal stresses.

	Perfect bond [MPa]	Interface film for bond reduction [MPa]
Reinforced ribs	65.54	2.35
Unreinforced ribs	97.13	8.62

which allow the slipping of the two materials (due to low mechanical properties of the interface i.e. polyurethane shear modulus G = 0.08 MPa).

The finite element model of the interface is shown in Fig. 18 with the results in the case of both perfect bonding and weak bond. Maximum shear stresses nearby the crack are significantly different. In the first case, the level of stress is 17.94 MPa, while in the second case the stress is negligible.

In addition, the amount of reinforcement plays a double role.

By increasing the reinforcement ratio, the restraint given by the reinforcement to the concrete is higher and thus cracking could occur earlier. Nevertheless, after cracking, the steel rebars play an important role bridging the cracks and ensuring the transmission of the internal forces.

Table 3 summarizes the results obtained in terms of maximum normal stress in the glass block near a shrinkage crack in the concrete.

The results show that the presence of both parameters is beneficial for the stress field in the glass block. The perfect bond causes a strong increase of the tensile stresses: the shear stresses distribution on the glass-concrete contact plane is characterized by a peak value of 17.94 MPa as reported in Fig. 18.

On the other hand, the effect of reinforcement is beneficial: nearby the crack, the bar is able to resist to tensile forces and to reduce the stresses in the glass block.

In the case of shrinkage cracks formation, tensile stress concentrations in the glass blocks are reduced thank to the crack bridging of the steel rebar that allows to transfer internal tensile forces throughout the cracks. Therefore, preventing significant shear stresses on the glass block to concrete interface and with a suitable reinforcement, shrinkage cracking would not be a major concern from a structural point of view. However, cracks in many cases may be a problem for aesthetic reasons.

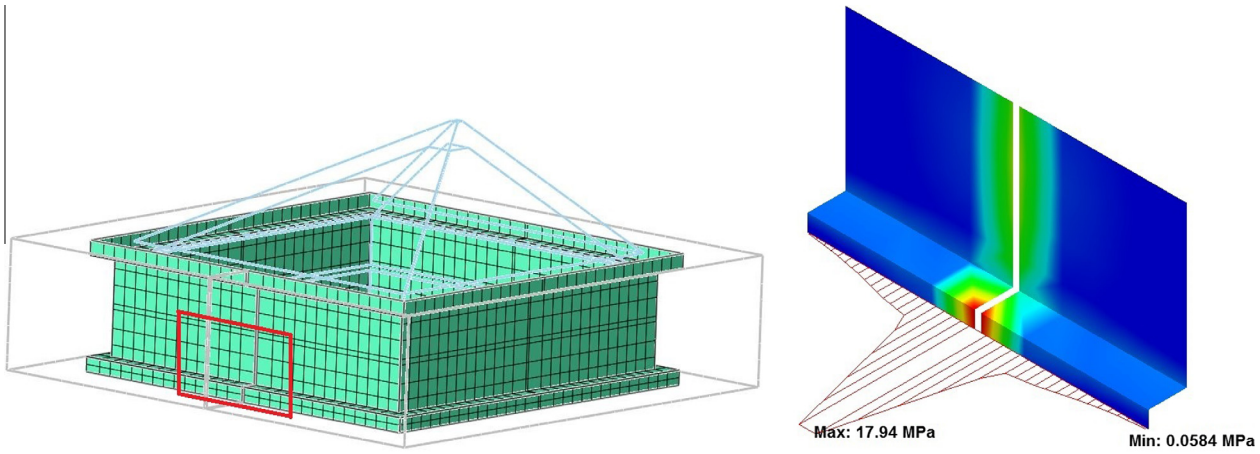

Fig. 18. Shear stresses on the interface for perfect bond: (a) position; (b) stresses distribution.

8. Conclusions

The damage of a glass-concrete façade panel was studied via 3D finite element numerical analyses considering the effect of concrete shrinkage and thermal loads due to the difference of temperature between outside and inside the building. The first phenomenon was identified as the main reason of the damage in glass blocks. Indeed, the restraint given by glass blocks and rebars caused high tensile stresses in concrete, much higher than the tensile strength of the material. Thus, the cracks developed and, as a consequence, the concrete stress release induced a tensile stress in glass blocks and rebars. The tensile stress in the glass blocks due to concrete cracking can be identified as the main cause of the observed damage.

The temperature effect is negligible with respect to the shrinkage effect.

For this reason, additional numerical finite element analyses, assuming as main factors concrete shrinkage strains and ribs size, have been performed and allowed to draw some advice to reduce the risk of damage in the glass bricks with different solutions.

- By adding SRA to the concrete mix the effect of shrinkage is mitigated, and it seems that concrete ribs up to 60 mm will not suffer any damage.
- The prescription suggested by glass block producers to realize ribs with limited size (about 15 mm) seems to be reasonable and seems to guarantee the glass block integrity even if SRA is not used.
- The bond between glass and concrete plays a primary role, by reducing it through adequate materials the tensile stress in glass blocks significantly drops.
- The reinforcement ratio should be properly chosen since it could be either detrimental or beneficial. Indeed a high amount of reinforcement could induce an earlier cracking due to the higher restraint. However, the rebars turn out helpful after concrete cracking because they allow the transmission of the internal forces.

From a practical point of view, every solution is associated with an economic impact; based on the importance of the element and the acceptable risk of damage it is possible to choose the most appropriate solution.

References

[1] A.J. Brookes, Cladding of Buildings, E & FN Spon, London (UK), 2002.
[2] R. Corrao, Glassblock and Architecture: evoluzione del vetro mattone e recenti applicazioni, Alinea Editrice, Firenze (I), 2010.
[3] B. Lawn, Fracture of Brittle Solids, second ed., Cambridge University Press, Cambridge (UK), 1993.
[4] M. Badalassi, L. Biolzi, G. Royer-Carfagni, W. Salvatore, Safety factors for the structural design of glass, Constr. Build. Mater. 55 (2014) 114–127.
[5] S. Cattaneo, F. Giussani, F. Mola, Flexural behavior of reinforced, prestressed and composite self-consolidating concrete beams, Constr. Build. Mater. 36 (2012) 826–837.
[6] S. Cattaneo, F. Mola, Assessing the quality control of self consolidating concrete properties, J. Constr. Eng. Manag. 138-2 (2012) 197–205.
[7] R.G. Colin, Cement and concrete as an engineering material: An historic appraisal and case study analysis, Eng. Fail. Anal. 40 (2014) 114–140.
[8] NTC 2008, Decreto Ministeriale 14/1/2008. Norme tecniche per le costruzioni. Ministry of Infrastructures and Transportations, G.U. S.O. n.30 on 4/2/2008, 2008 (in Italian).
[9] EN 1051-2, Glass in Building. Glass Blocks and Glass Pavers – Part 2: Evaluation of Conformity/Product Standard. Brussels, 2007.
[10] EN 673, Glass in Building – Determination of Thermal Transmittance (U value) – Calculation Method. Brussels, 2005.
[11] EN 1051-1, Glass in Building. Glass Blocks and Glass Pavers – Part 1: Definitions and Description. Brussels, 2003.
[12] EN ISO 7459, Glass Containers – Thermal Shock Resistance and Thermal Shock Endurance – Test Methods. Brussels, 2004.
[13] EN ISO 8339, Building Construction – Sealants – Determination of Tensile Properties. Brussels, 2005.
[14] FIB Model Code for Concrete Structures 2010, Ernst & Sohn pub., 2013.
[15] B.J. Pease, The role of shrinkage reducing admixtures on shrinkage, stress development and cracking, Faculty of Purdue University, 2005 (PhD dissertation).
[16] P. Rossi, J. Tailhan, F. Le Maou, Comparison of concrete creep in tension and in compression: Influence of concrete age at loading and drying conditions, Cem. Concr. Res. 51 (2013) 78–84.
[17] N. Ranaivomanana, S. Multon, A. Turatsinze, Basic creep of concrete under compression, tension and bending, Constr. Build. Mater. 38 (2013) 173–180.